

Study of mangrove tannin and flavanoid monomers as alternative steel corrosion inhibitors in acidic medium

Afidah A. Rahim^{a,*}, E. Rocca^b, J. Steinmetz^b, M.J. Kassim^a, R. Adnan^a, M. Sani Ibrahim^a

^a*School of Chemical Sciences, University Sains Malaysia, 11800 Penang, Malaysia*

^b*Laboratoire de Chimie du Solide Mineral – Universite Henri Poincare – Nancy I BP 239 – 54506 Vandoeuvre Les Nancy – France*

Abstract

The inhibitive behaviour on steel of flavanoid monomers that constitute mangrove tannins namely catechin, epicatechin, epigallocatechin and epicatechingallate was investigated in an aerated HCl solution via electrochemical methods. The monomers were found to be mainly cathodic inhibitors and the inhibition efficiency dependent on concentration. To explain the adsorptive behaviour of the molecules on the steel surface, a semiempirical approach involving quantum chemical calculations using HyperChem 6.0 was undertaken. The correlation between the electronic density of the molecule and the inhibiting properties was established. The most probable adsorption centers were found in the vicinity of the phenolic groups. In a second part, the use of mangrove tannin, extracted from the mangrove barks as steel corrosion inhibitors in acidic media was investigated and its inhibitive efficiency was compared with that of commercial mimosa, quebracho and chestnut tannins. The inhibitive performance of mangrove tannin was comparable to the other tannins investigated, indicating its potential in corrosion protection.

Keywords: F. Flavanoids; I. Inhibition efficiency; M. Molecular modelling, T. Tannin

* Corresponding author. Fax: +6046574854
E-mail address: afidah@usm.my

1.0 Introduction

In many industries, the need to use constructional materials safely, but cost-effectively, is a primary consideration. Frequently, physical requirements can be satisfied easily, but corrosion effects seriously complicate the selection of suitable materials. Generally, increased corrosion-resistance can only be obtained at increased cost. However, the actual material-related costs incurred in a project will depend on the corrosivity of the environment concerned, the required design life, the physical requirements of the material, and the readily available stocks. The costs and problems associated with corrosion-resistant materials means that, in many cases, the use of corrosion inhibitors is a practical and economic alternative. Industrial use of corrosion inhibitors is, therefore, now broad based and extensive.

Most of the well known acid inhibitors are organic compounds that contain nitrogen, sulphur, oxygen and multiple bonds in the molecules which are adsorbed on the metal surface and these compounds have continued to provoke research interests [1-11].

Tannins, a class of natural, non-toxic and biodegradable polyphenolic compounds, extracted from plant sources are already in use as corrosion inhibitors in aqueous media, components of rust converters, pigments in paint coatings, corrosion inhibitors of reinforcing steel in concrete, chemical cleaning agents for removing iron-based deposits and oxygen scavengers for boiler water treatment system. Tannins are divided into two classes of polymers, the hydrolysable tannins and the condensed tannins. The hydrolysable tannins are gallic and/or egallic acid which easily hydrolyse in acidic media. Condensed tannins are polymeric flavanoids. Hydrolysable tannin, mainly from a chestnut tree, condensed tannin such as the mimosa tannin from the

wattle tree and tannins comprising of hydrolysable and condensed tannin such as the oak tannin have long been the subject of inhibition studies [12-19].

Tannins as corrosion inhibitors are applied both in solvent and waterborne pretreatment formulations. These formulations could be applied on partially rusted substrates, reducing the effort needed for cleaning the surface by sandblasting or other methods which proved to be expensive and are not applicable in many situations.

They have been called rust converters since their presence converts active rust into compounds that are more stable and corrosion resistant. A rapid reaction was found to occur between rusty iron and natural tannins. The transformation of rusty iron into the blue-black coating layer has been attributed to the complexation of the polyphenolics moiety of the tannin to the iron oxides and oxyhydroxides. Although other complexation products undoubtedly formed, the ferric tannate complex has been cited as the major product. However the protective efficiency of ferric-tannate against further corrosion generated contradictory opinions. According to Pardini et al.[19] and Matamala et al. [20], tannins are more effective when used in conjunction with phosphoric acid. On the other hand, DesLauriers [21] found the efficiency of this type of pretreatment to be inadequate. Due to the diversity of the material used in different studies, different explanations on the inhibitory mechanisms have been suggested and despite the long and extensive studies of various tannin extracts in metallic corrosion inhibition and protection, little is known about the corrosive efficiency of mangrove tannins.

A reversed-phase HPLC analysis of the mangrove tannins have shown that the mangrove tannins constitute mainly of four flavanoid monomers namely catechin, epicatechin, epigallocatechin and epicatechin gallate [22]. The structures of these monomers are as shown in Fig. 1. In this study, the inhibitive behaviour on steel of

these monomers was investigated in an aerated HCl solution via electrochemical methods. The adsorptive behaviour of these monomers on steel will be explained using a semiempirical approach involving quantum chemical calculations. In a second part, the study of mangrove tannins as corrosion inhibitors was undertaken and the inhibitive efficiency of flavanoid monomers was compared with that of mangrove tannins and commercial mimosa, quebracho and chestnut tannins.

2. Experimental details

2.1 Tannin isolation

Mangrove bark samples (*Rhizophora apiculata*) were obtained from the Matang Forest, Malaysia. The extraction of tannins from mangrove barks was carried out by total immersion of finely ground barks in 70% aqueous acetone for 72 hours at room temperature. The acetone was removed under pressure and the resulting aqueous fraction was freeze-dried, yielding 25-27% weight of the dry barks. Mimosa, quebracho and chestnut tannins were obtained from SILVACHIMICA, Italy.

2.2 Electrochemical studies

Electrochemical tests were carried out in a three-electrode electrochemical cell connected to an EGG Princeton 263A or 273A potentiostats. A circular and horizontal working electrode was placed at the bottom of the cell under a Pt-disk electrode. Acquisition of data and calculation of electrochemical parameters were done by a 352 Soft Corr software. The reference electrode was a KCL-saturated calomel electrode ($E=0.241$ V/NHE), and all working electrode potentials are measured versus this reference electrode. The electrochemical corrosion tests were carried out using steels for automotive applications provided by Arcelor. Prior to each experiment, the

electrodes were polished mechanically on a Struers Rotopol-2 polishing machine using SiC paper of 120, 400 and up to a final 1200 grit. After rinsing with distilled water, the test electrodes were cleaned with alcohol and dried in air, then immediately immersed in the aerated test solution. The following experiment sequence was used:

- (i) Measurement of the corrosion potential (E_{corr}) and the polarisation resistance (R_p), performed every 1 h 30 minutes for a duration of 18 h, with a scan rate of 0.166 mV/s for a range ($E_{corr} \pm 20$ mV).
- (ii) Recording the potentiodynamic curve, $i=f(E)$, from -300 to 300 mV versus E_{corr} with a sweep rate of 1 mV/s.

Test solutions containing catechin, epicatechin, epigallocatechin and epicatechin gallate monomers (Sigma chemicals) ranging from 1.0×10^{-3} M to 5×10^{-2} M were prepared in 25v% ethanolic 0.5M HCl. A 25v% ethanolic 0.5 M HCl solution was used as the standard solution. Test solutions containing mangrove tannin ranging from 0.1 g/L to 6.0 g/L were prepared by diluting the tannin sample in a 0.5 M HCl solution. The pH of the solution was adjusted to pH 0.5. A 3 g/L mimosa tannin, quebracho tannin and chestnut tannin were used for subsequent studies. The pH of the solutions was increased by the addition of NaOH solutions. The electrochemical tests were carried out at pH 0, 0.5, 2.0 and 4.0. Pre-rusted coupons (2.5 cm x 3.5 cm) which were prepared by immersion in 3.5% NaCl solution for 35 days at room temperature (20 °C) resulted in an average rust thickness of 2.60 mg/cm². These coupons were immersed in 5 g/L mangrove tannin solution at pH 4.0 and for 24 h. The surface morphology was determined by SEM analysis using SEM S-2500 Hitachi Thermo NORAN equipped with an energy-dispersive X-ray spectrometer.

2.3. Molecular modelling

Quantum chemical calculations were performed using HyperChem 6.0 package. A PM3 semi-empirical parameterisation was used to obtain the geometry optimisation of the flavanoids. The potential energy minimum was obtained from the steepest descent algorithm and the iteration terminated when the RMS energy gradient reached 1×10^{-2} kcal $\text{\AA}^{-1} \text{mol}^{-1}$. Single point calculation was used to determine the molecular properties of the flavanoids with minimum energy conformation.

2.4. Synthesis of ferric-tannates

The ferric-tannates were prepared by the addition of 40 mL 6 g/L tannin solution and 10 mL 0.1 M ferric ammonium sulphate, $\text{FeNH}_4(\text{SO}_4)_2 \cdot 12\text{H}_2\text{O}$ (Fluka) solution at pH 4.0. The mixture was mechanically stirred and left to react at room temperature for one day. The mixture was then centrifuged for 20 minutes. The ferric-tannate complex was collected, washed and freeze-dried. A Perkin Elmer System 2000 spectrometer was used to obtain the FTIR spectrums of the ferric complex.

2.5. Analysis of reducing power

Standard L(+) ascorbic acid (Merck) solution of concentrations 2.0×10^{-2} mg/mL – 0.1 mg/mL were prepared. To 1.0 mL of the standard solution, 2.5 mL of 0.2 M phosphate buffer at pH 6.6 (prepared from the addition of 0.2 M Na_2HPO_4 and 0.2 M NaH_2PO_4) (AJAX chemicals) and 2.5 mL of 1% (w/v) potassium ferricyanide, $\text{K}_3\text{Fe}(\text{CN})_6$ (Fluka) solution were added. The mixture was incubated at 50 °C for 20 minutes after which 2.5 mL 10%(w/v) trichloroacetic acid (ACROS) was added. The resultant mixture was centrifuged for 20 minutes at 2500 rpm. The upper layer (2.5 mL) was dispensed and 2.5 mL distilled water and 0.5 mL of 0.1%(w/v) ferric chloride hexahydrate, $\text{FeCl}_3 \cdot 6\text{H}_2\text{O}$ (Fluka) solution were added. The absorbance was

measured at 700 nm. The procedure was repeated for (+)-catechin hydrate (Fluka) standard solutions, mangrove, mimosa, quebracho and chestnut tannins (SILVACHIMICA, Italy).

3. Results

3.1. Inhibition efficiency of flavanoid monomers in 0.5 M HCl

From the results of the inhibitory performance of the monomers via electrochemical tests, it was found that all monomers cause some degree of inhibition for concentrations as low as 2.5×10^{-3} M. The potentiodynamic curves of steel in 0.5 M HCl containing catechin, epicatechin, epigallocatechin and epicatechin gallate are as shown in Fig. 2. The inhibitory performance was found to be dependent on concentration as witnessed from the different responses of the individual monomers with respect to concentration. Interestingly, one can observe that all monomers exhibited shifts in the cathodic curves to lower density currents at all concentrations, resulting in more negative E_{corr} values, thereby categorising the monomers as cathodic inhibitors. The cathodic Tafel slope of ~ 110 mV/decade and the anodic slope of ~ 100 mV/decade corresponding to the reduction of H^+ to hydrogen, H_2 and oxidation of Fe to Fe^{2+} respectively, remained unchanged after the addition of the various concentrations of monomers. Figure 3 shows the R_p evolution with immersion time. At a concentration of 2.5×10^{-3} M, R_p values decreased slightly with time of immersion for all monomers. With the exception of epigallocatechin, the R_p values at a concentration of 5.0×10^{-3} M initially decreased to a certain point, and after 10 hours of immersion, the R_p slowly increased. At the higher concentration of 1.0×10^{-2} M, the R_p for catechin reduced to reach a minimum after 9 hours of immersion, after which the R_p then increased, reaching a plateau after 13.5 hours. The R_p for all the

other monomers initially reduced and finally remained constant after 7.5 hours.

Epicatechingallate, epicatechin and catechin gave the highest R_p at 2.5×10^{-3} M, 5.0×10^{-3} M and 1.0×10^{-2} M respectively throughout 18 hours of immersion. Nevertheless, the R_p values have the same order of magnitude for all monomers, indicating the same inhibition efficiency.

Table 1 lists the inhibition efficiency, $IE(\%)$ calculated by the polarisation resistance according to the following equation:

$$IE(\%) = \frac{R_p - R_{p_0}}{R_p} \times 100 \quad (1)$$

Where R_{p_0} and R_p are the uninhibited and inhibited polarisation values respectively. For almost all the monomers investigated, a maximum inhibition of more than 70% was achieved. Catechin produced inhibition of between 56%-69% and a maximum was reached at 1.0×10^{-2} M. A wider variation of inhibition efficiency of 33%-72% was observed for epicatechin with the highest value at 5.0×10^{-3} M. On the other hand, for epicatechin gallate a decrease in efficiency as the concentrations increased was observed, attaining 74% inhibition at the lowest concentration of 2.5×10^{-3} M. Due to the scarcity of epigallocatechin, inhibition efficiency investigated was limited to concentrations up to 5.0×10^{-3} M, with a maximum inhibition of 65% at this concentration. On the whole, the monomers produced more than 50% inhibition for concentrations of 1.0×10^{-2} M and below.

3.2 Molecular modelling of flavanoid monomers

The effectiveness of a corrosion inhibitor can be related to its molecular spatial structure and molecular electronic structure in addition to its hydrophobicity, solubility and dispersibility [23-25]. An example of an optimised molecular structure

of a catechin monomer with its HOMO density is as shown in Fig. 4(a). The highest values of the electron density of the frontier orbital were found within the vicinity of the A aromatic ring. Conversely, for epicatechin (Fig. 4(b)) and epigallocatechin (Fig. 4(c)) the highest values of the electron density of the frontier orbital were found within the vicinity of the B aromatic ring.

3.2. Inhibition efficiency of tannins

Fig. 5 shows the effect of concentration on the inhibitory performance of mangrove tannins. Although no inhibition effect was observed after the addition of 0.1 g/L tannin, a gradual decrease of the same gradient in the cathodic curves were observed as the tannin concentration increased from 1 g/L to 6 g/L. This suggests that the mechanism of the hydrogen evolution reaction was the same as these concentrations were increased. From the potentiodynamic curves, it is clearly seen that the I_{corr} decreases as the concentration increases indicating that with the increase in concentration of tannin, more tannin molecules are being adsorbed on to the surface of the metal, enhancing more uniform surface coverage, which decreases the cathodic reaction rate of the hydrogen reduction. Table 2 lists the inhibition efficiency, $IE(\%)$ based on I_{corr} from the Tafel curves which was calculated according to the following equation :

$$IE(\%) = \frac{I_{corr_o} - I_{corr}}{I_{corr_o}} \times 100 \quad (2)$$

Where I_{corr_o} and I_{corr} are the uninhibited and inhibited corrosion current densities respectively and R_p measurements (calculated from equation 1) of mild steel in 0.5 M HCl containing the various concentrations of mangrove tannins. The inhibition efficiency calculated using both methods was found to be similar. A gradual increase

in efficiency as the concentrations of mangrove tannin were increased was observed. More than 80% inhibition was achieved with 3g/L and 6 g/L of mangrove tannins. Our studies have also shown that corrosion rate was also reduced in HCl solution at pH 0, 2.0 and 4.0 in the presence of 3 g/L mangrove tannin.

The inhibitive efficiency of mangrove tannin was also compared with the condensed tannin of mangrove which was extracted according to a procedure as described elsewhere [26] and the results are as depicted in Table 3. The condensed tannin of mangrove shows a decrease in the percentage inhibition with increasing pH, similar to the entire mangrove tannin. The small percentage difference between the entire mangrove tannin and condensed tannin indicated that the inhibition is predominantly provided by the condensed tannin substituent of mangrove tannin.

The similarity in tannin behaviour is reflected in the electrochemical studies. From our study it was found that the potentiodynamic curves of mimosa, quebracho and chestnut tannins exhibited shifts in the cathodic curves to lower density currents similar to mangrove tannin at pH 0, 0.5 and 2.0, signifying that all tannins act as cathodic inhibitors. Table 3 represents the inhibition efficiency, $IE(\%)$ based on I_{corr} and R_p measurements for mild steel in HCl containing the various tannins at pH 0, 0.5, 2.0 and 4.0. Regardless of whether the inhibition efficiency was calculated from I_{corr} from the potentiodynamic curves or R_p measurements, all tannins show a similar pattern of a decrease in efficiency with the increase in pH. More than 80% inhibition efficiency was achieved at pH 0 and 0.5 for all tannins. A drastic reduction in efficiency was observed for chestnut tannin as the pH increased from pH 0.5 to 2.0. While at pH 0.02 and 0.5 all tannin have almost the same efficiency, the efficiency decrease in the order of mimosa tannin > mangrove tannin > quebracho tannin > chestnut tannin at pH 2.0.

3.4 Surface analysis

The surface observation of steel after immersion in tannin solutions at pH 0 revealed no deposit and a clean iron aspect. In contrary at higher pH (2 and 4) a blue-black precipitate typical to that of ferric-tannate is observed. Indeed, FTIR experiments show similar spectrums for the blue-black deposit and the ferric-tannates synthesised from the reaction of mangrove tannins and ferric salt at pH 4.0.

The tannin spectrum (Fig. 6) shows a broad absorption band between 3700 and 2700 cm^{-1} which is due to the presence of hydroxyl groups. Three peaks occurring at 1600, 1521 and 1447 cm^{-1} are characteristic of aromatic compounds. Various peaks in the 600 to 900 cm^{-1} and smaller peaks between 1000 and 1300 cm^{-1} correspond to substituted benzene rings. For the ferric-tannate spectrum, several of the peaks not only shifted slightly, but reduced in intensity. The reduced intensity of the broad peak at around 3300 cm^{-1} designates the reduction of free OH groups [16] since it is the proximity of hydroxyl groups on the aromatic rings which enable the tannins to chelate iron ions. The amorphous character of the deposit and the synthesised ferric-tannates was shown by XRD experiments.

3.5 Reducing power of tannins

It is believed that flavanoid monomers and tannins are antioxidant species [27-31] characterised by a reducing power. The reducing power of mangrove tannins was confirmed from the method proposed by Gulcin et al. [27] after a slight modification. In this procedure, $\text{Fe}(\text{CN})_6^{3-}$ ions will be reduced to $\text{Fe}(\text{CN})_6^{4-}$ ions when a reductant is added. The ferric chloride solution will then react with these ions to form $\text{Fe}_4[\text{Fe}(\text{CN})_6]_3$ complex. The Fe^{2+} present in the complex will be detected at 700 nm. Thus, increased absorbance indicates increased reducing power. The results of the

reducing power determination are as shown in Fig. 7. The reducing power of mangrove tannin increased slightly as the concentration increased to 6.0×10^{-2} mg/mL, after which it reached a plateau. While mimosa tannin exhibited the same behaviour as mangrove tannin, the reducing power of quebracho tannin and chestnut tannin continued to increase slightly as the concentrations were increased. Although the reducing power of mangrove tannin falls far below that of ascorbic acid standard and slightly below the catechin standard, the reducing power is comparable with that of catechin at the lower concentrations (2.0×10^{-2} mg/mL and 4.0×10^{-2} mg/mL) and other commercial tannins investigated.

The complexing and reducing power of tannins is further affirmed by the transformation of the morphology of pre-rusted iron after the addition of mangrove tannins as shown by the SEM micrographs in Fig. 8. The pre-rusted sample which was found to consist of mainly lepidocrocite (γ -FeOOH) and magnetite (Fe_3O_4) as confirmed by X-ray diffractions, shows basically flower-like flakes with finger-like structures protruding in a random manner. The transformation of rust into blue-black ferric-tannate deposits gave rise to a coarse layer of cracks with irregular shapes, more rounded than angular. The edges seem to lift from the surface indicating the lack of adhesion.

4. Discussion

The electrochemical studies have shown that all flavanoid monomers investigated have an interesting behaviour of cathodic inhibition in very acidic media. Comparison of the inhibition efficiency of the monomers at the same concentration, the inhibition efficiencies decrease in the order of epicatechin gallate > catechin > epigallocatechin >

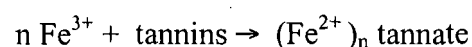
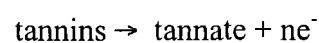
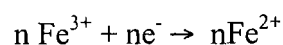
epicatechin at 2.5×10^{-3} M, epicatechin > epigallocatechin > epicatechin gallate > catechin at 5.0×10^{-3} M and catechin > epicatechin gallate > epicatechin at 1.0×10^{-2} M. Thus, the dependency of inhibitory performance of the monomers on concentration is clearly evident. In 0.5 M HCl, the inhibitive property of flavanoid monomers is due to the chemisorption of the flavanoid molecules onto the surface which was revealed by our surface observation and reported by Martinez and Stern [12,13]. From the molecular modelling, it was found that adsorption of flavanoid molecules could take place on either A or B aromatic ring depending on the orientation of the flavanoid monomer and the number of phenolic groups attached to the molecule. Adsorption could therefore proceed via sharing of the donor group (-OH) electrons or aromatic π -electrons, between the flavanoid molecule and the partially filled d-orbitals of iron. According to Pearson's hard and soft acid and base (HSAB) principle, hard acids prefer to bind to hard bases and soft acids prefer to bind to soft bases. When the HOMO-LUMO energy gap is small, this results in electron transfer from donor base atom to acceptor atom in the acid molecule and the resulting compound is covalent in nature. Thus soft-soft interactions are frontier-controlled [32]. All the flavanoid molecules investigated gave rise to HOMO-LUMO energy gap of 8.92-9.12 eV, signifying soft acid-soft base interaction between iron metal and flavanoid molecule. This leads to the fact that since bulk metals are soft acids, flavanoid molecules as soft base inhibitors are most effective for metals corroding in acidic medium [14]. This is indeed consistent with the results obtained via the electrochemical studies which indicated various degree of inhibition by the flavanoid monomers in acidic solution. Although the molecular modelling shows two different sites of adsorption, these two sites have equal absorption efficiency according to the electrochemical measurements.

As observed for catechin, epicatechin and epicatechin gallate, the decrease of the inhibition efficiency with the increase of monomers concentration can be explained by the formation of soluble oligomers, causing a secondary desorption from the substrate [4].

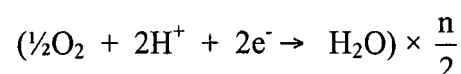
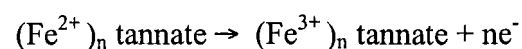
Similar inhibition behaviour of tannins was observed at all pH. The inhibitive property of tannins at pH 0 and 0.5 could be due to the chemisorption of the tannin molecules onto the surface similar to the flavanoid monomers. Nevertheless, it could be noted that when the flavanoid monomers were used individually a maximum of ~70% inhibition was achieved. Thus a combination of these monomers are required to enhance individual's capacity, producing a synergistic effect in attaining more than 80% inhibition produced by condensed tannins and entire mangrove tannins.

At higher pH, the cathodic action of tannins decreases, but they are able to complex with Fe^{2+} ions to form ferrous-tannates which can be easily oxidised into ferric-tannates, a blue-black deposit when in contact with oxygen. Thus tannins inhibit the oxidation of Fe^{2+} ions into ferric oxides/oxyhydroxides (Fe_3O_4 , $FeOOH$) and avoid the formation of red rust.

Indeed, our results also show the ability of tannins to reduce Fe^{3+} ions into ferrous-tannates. Schematically, it is proposed:



Consequently,





The reducing power of tannins allows the inhibition of Fe^{3+} -oxyhydroxides formation on clean steel surfaces and the Fe^{3+} -oxyhydroxides are instead transformed into Fe^{3+} -tannates. Although several authors claim a protective effect of this deposit [15-20, 33, 34], our results indicated a low protective behaviour.

5. Conclusion

1. The electrochemical study has shown that the flavanoid monomers that constitute mangrove tannin are potential inhibitors for steel in acidic medium.
2. All monomers act mainly as cathodic inhibitors of the steel corrosion and its inhibitive performance dependent on concentration in acidic conditions.
3. Molecular modelling has shown that adsorption of flavanoids occurs within the vicinity of the phenolic groups on either A or B aromatic ring. There is no preferential site which explains the equal inhibition performance of monomers. The study also shows that the monomers are effective inhibitors for corroding metals in acidic medium.
4. All tannins investigated are cathodic inhibitors and the inhibition efficiency of all tannins was found to decrease with increasing pH.
5. The inhibitive performance of mangrove tannin is comparable with that of commercial mimosa, quebracho and chestnut tannins at pH 0, 0.5 and 2.0 and shows superiority over the rest of the tannins at pH 4.0.

6. References

1. A.K. Maayta, N.A.F. Al-Rawashdeh, *Corrosion Science*, 46, (2004) 1129.
2. W. Hui-Long, L. Rui-Bin, X. Jian, *Corrosion Science*, 46, (2004) 2455.
3. P. Morales-Gil, G. Negron-Silva, M. Romero-Romo, C. Angeles-Chavez, M. Palomar-Pardave, *Electrochimica Acta*, 49, (2004) 4733.
4. M. Ozcan, I. Dehri, M. Erbil, *Applied Surface Science*, 236, (2004) 155.
5. R. Ravichandran, S. Nanjundan, N. Rajendran, *Applied Surface Science*, 236, (2004) 241.
6. E. S. Ferreira, C. Giacomelli, F.C. Giacomelli, A Spinelli, *Materials Chemistry and Physics*, 83, (2004) 129.
7. A. Lgamri, H. A. El Makarim, A. Guenbour, A. B. Bachir, L. Aries, S. El Hajjaji, *Progress in Organic Coatings*, 48, (2003) 63.
8. M. Hosseini, S. F.L. Mertens, M. Ghorbani, M. R. Arshadi, *Materials Chemistry and Physics*, 78, (2003) 800.
9. M.M. Osman, R.A. El-Ghazawy, A.M. Al-Sabagh, *Materials Chemistry and Physics*, 80, (2003) 55.
10. V. Branzoi, F. Golgovici, F. Branzoi, *Materials Chemistry and Physics*, 78, (2002) 122.
11. M. Lagrenee, B. Mernari, M. Bouanis, M. Traisnel, F. Bentiss, *Corrosion Science*, 44, (2002) 573.
12. S. Martinez, I. Stern, *Journal of Applied Electrochemistry*, 31, (2001) 973.
13. S. Martinez, I. Stern, *Applied Surface Science*, 199, (2002) 83.
14. S. Martinez, *Materials Chemistry and Physics*, 77, (2002) 97.
15. T.K. Ross, R.A. Francis, *Corrosion Science*, 18, (1978) 351.

16. J. Gust, *Corrosion*, 47, (1991) 453.
17. J. Gust, J. Bobrowicz, *Corrosion*, 49, (1993) 24.
18. J. Gust, J. Suwalski, *Corrosion Science*, 50, (5), (1994) 355.
19. O.R. Pardini, J.I. Amalvy, A.R.Di Sarli, R. Romagnoli, V.F. Vetere., *J.Coat. Technol.*,73, (2001) 99.
- 20 G. Matamala, W. Smeltzer, G. Droguett, *Corrosion*, 50, (1994) 270.
21. P.J. Deslauriers, *Material Performance*, 26, (1987) 35.
22. A. Abdul Rahim, E. Rocca, J. Steinmetz, R. Adnan, M.J. Kassim, *Proceeding of the European Corrosion Conference(EUROCORR 2004) Paper No. 041, 2004.*
23. V.S. Sastri, J.R. Perumareddi, *Corrosion*, 50, (1994) 432.
24. V.S. Sastri, J.R.Perumareddi, *Corrosion*, 53, (1999) 671.
25. I. Lukovits, E. Kalman, F. Zucchi, *Corrosion*, 57 (2001) 3.
26. Afidah Abdul Rahim, Henny Sumilo, Jain Kassim, Sani Ibrahim, "Separation and Identification of Mangrove Condensed Tannin", presented in the Simposium Kimia Analisis Ke-15,(SKAM 15), 10-12 September, Penang, Malaysia, (2002).
27. I. Gulcin, M. Oktay, E. Kirecci, O. I. Kufrevioglu, *Food Chemistry*, 83, (2003) 371.
28. C. A. Rice-Evans, N. J. Miller, G. Paganga, *Free Radical Biology & Medicine*, 20, (7), (1996) 933.
29. S. Mi-Yea, K. Tae-Hun, S. Nak-ju, *Food Chemistry*, 82, (2003) 593-597.
30. K. Kondo, M. Kurihara, N. Miyata, T. Suzuki, M.Toyoda, *Archives of Biochemistry and Biophysics*, 362, (1), (1999) 79.
31. N. Salah, N. J. Miller, G. Paganga, L. Tijbourg, G. P.Bolwell and C. Rice-Evans, *Archives of Biochemistry and Biophysics*, 322, (2), (1995) 339.

32. V.S. Sastri, Corrosion Inhibitors. Principles and Applications. John Wiley & Sons, England, 1998.
33. E. Ivanov, Y.I. Kuznetsov, Zashchita Metallov, 26, (1), (1990) 48.
34. E. Ivanov, Y.I. Kuznetsov, Zashchita Metallov, 27, (3), (1991) 379.

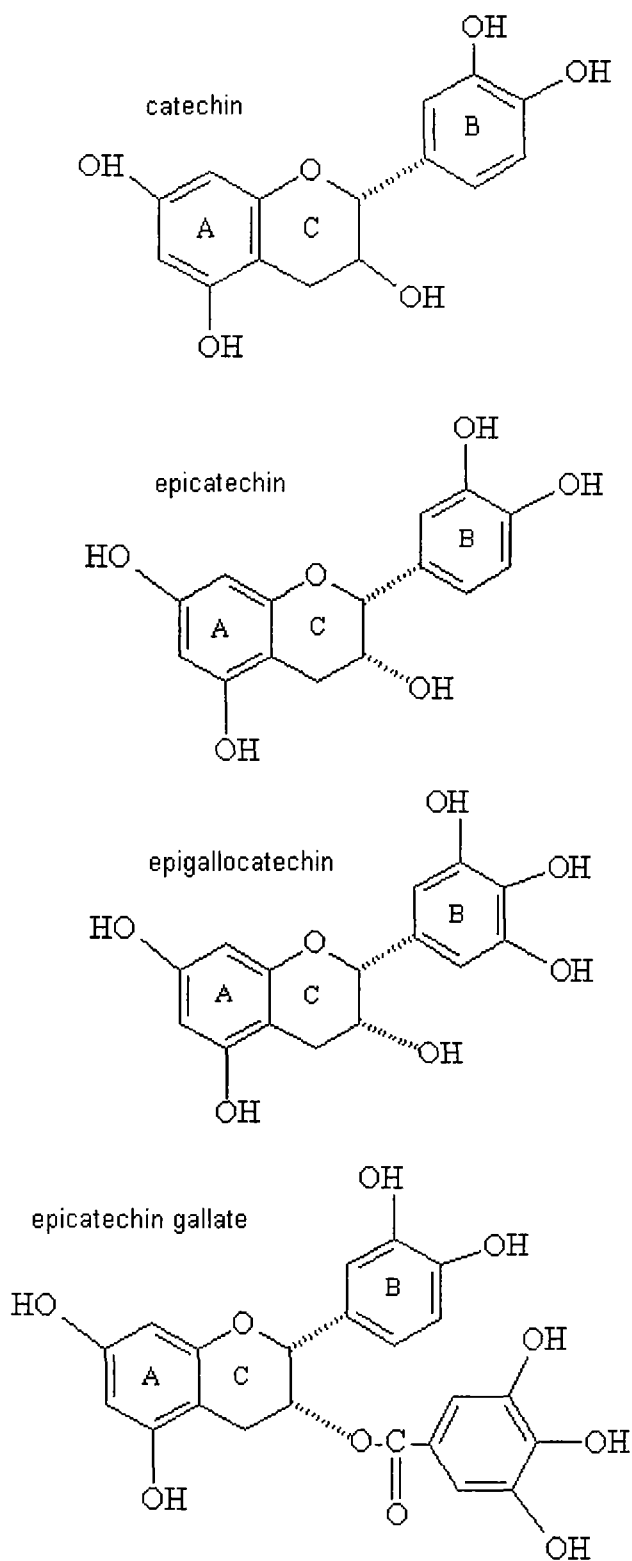
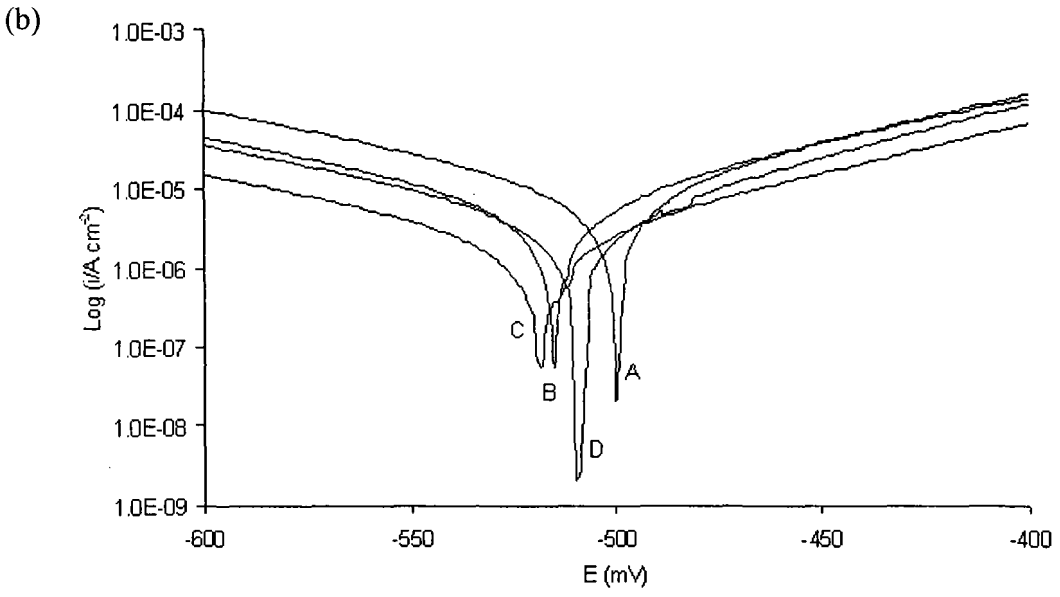
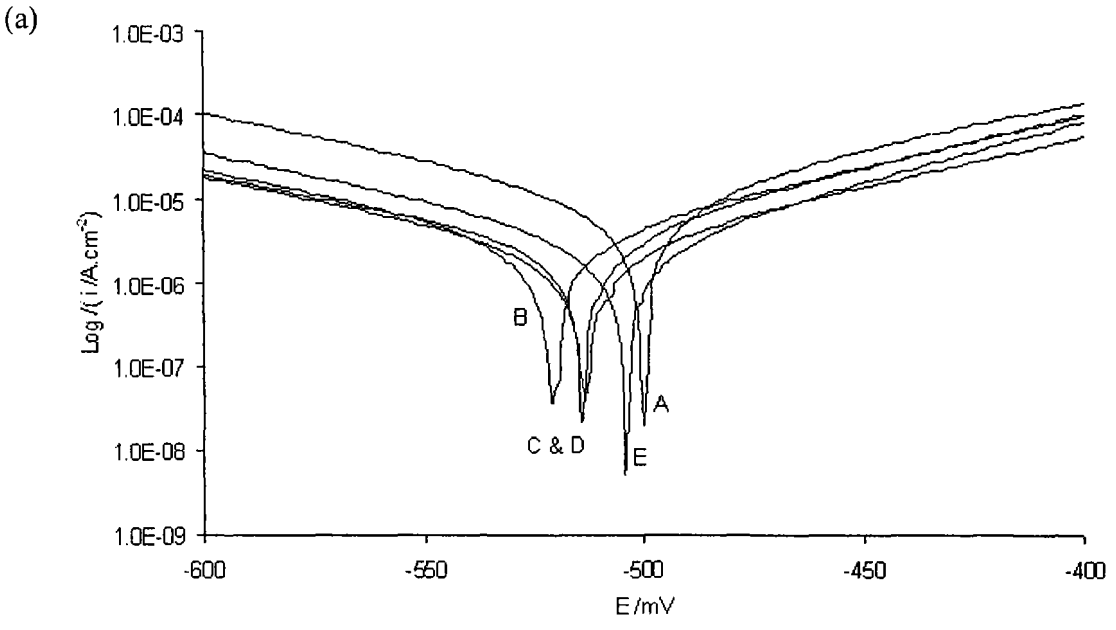


Fig. 1. Chemical structure of flavanoid monomers that constitute mangrove tannin.



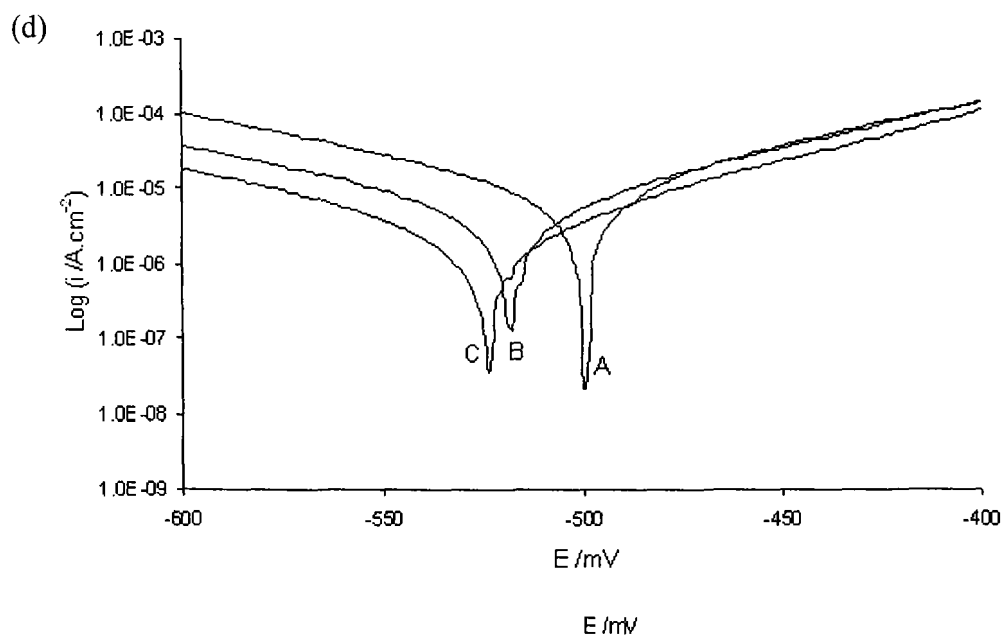
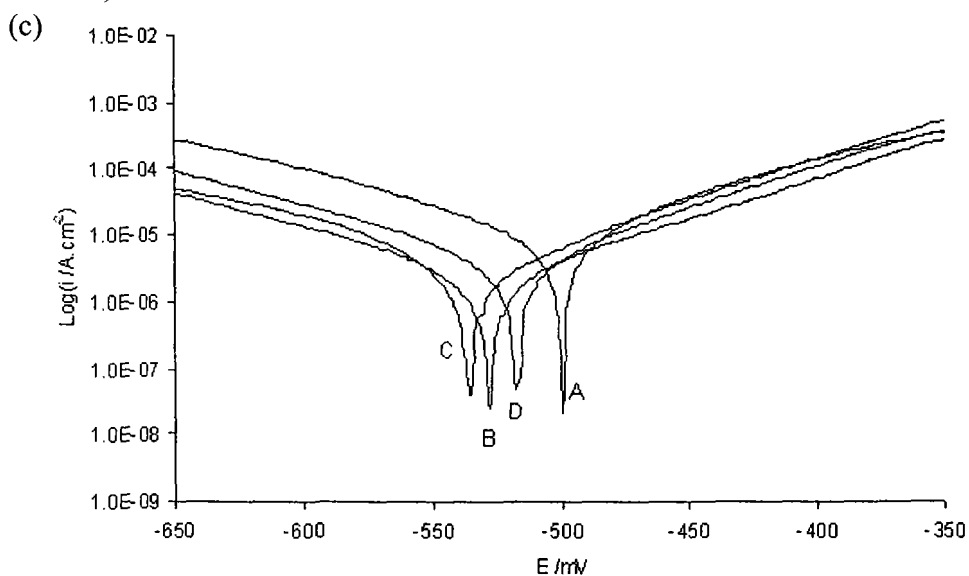
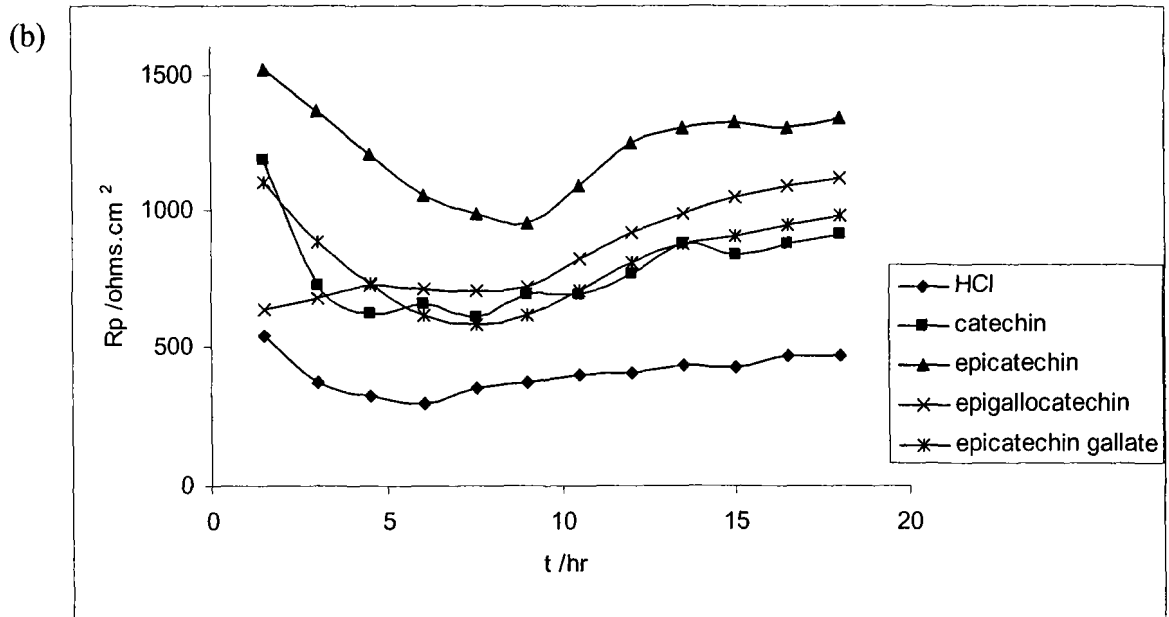
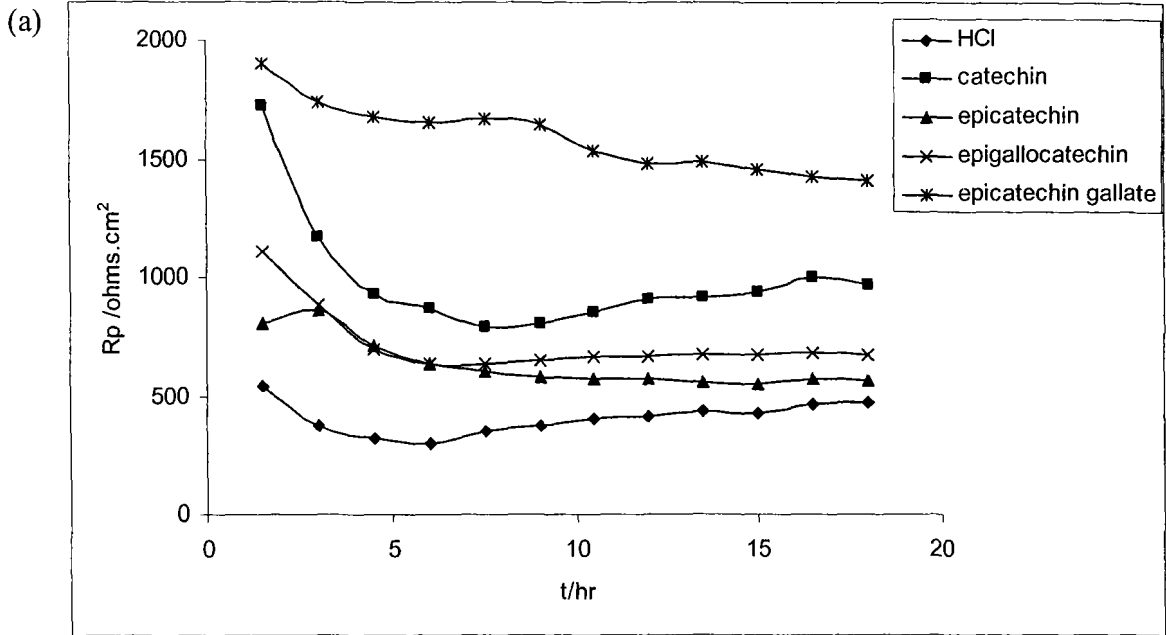


Fig. 2. Potentiodynamic curves of steel in 0.5 M HCl containing various concentrations of (a) catechin, (b) epicatechin, (c) epicatechin gallate and (d) epigallocatechin: A- HCl solution, B- 2.5×10^{-3} M, C- 5.0×10^{-3} M, D- 1.0×10^{-2} M, E- 5.0×10^{-2} M.



(c)

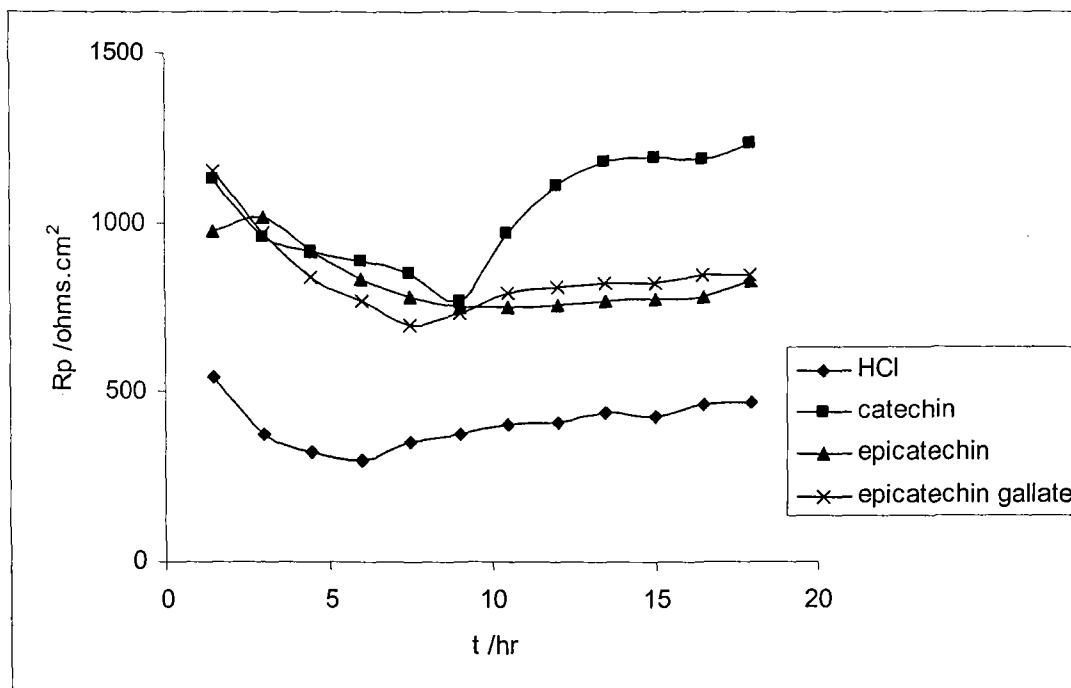
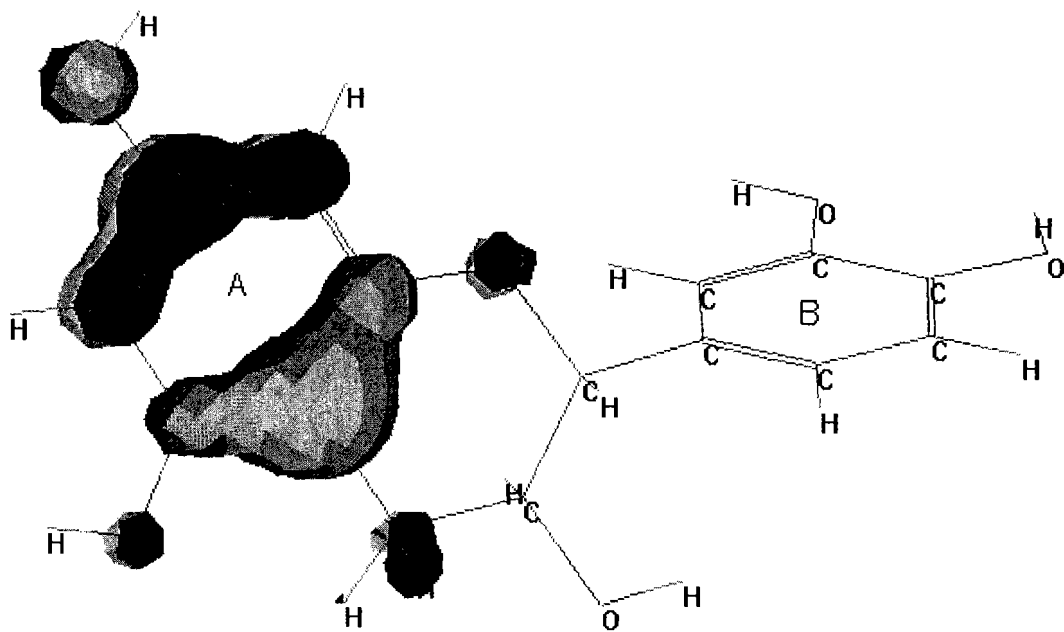
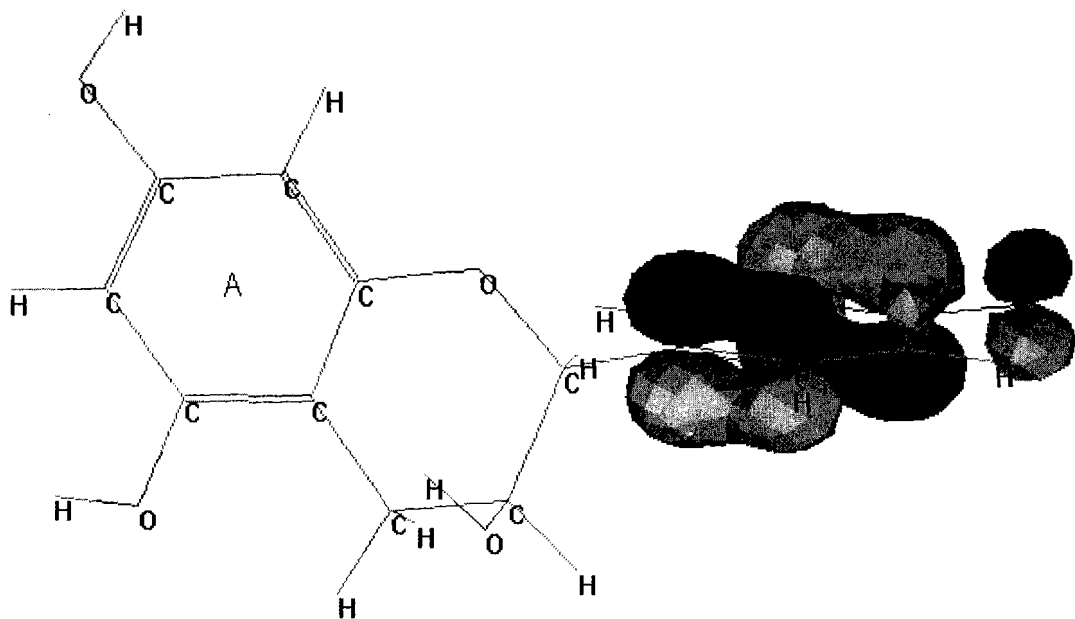


Fig. 3. Variation of polarisation resistance, R_p with time of immersion containing (a) 2.5×10^{-3} M, (b) 5.0×10^{-3} M and (c) 1.0×10^{-2} M flavanoids in 0.5 M HCL.

(a)



(b)



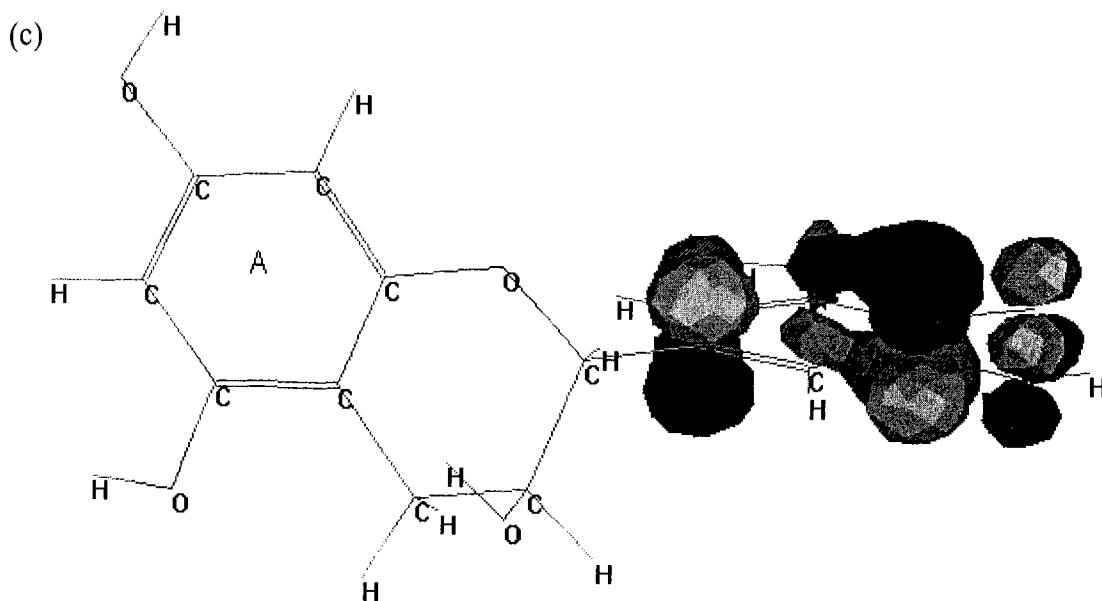


Fig. 4. HOMO density as an isosurface for (a) catechin, (b) epicatechin and (c) epigallocatechin monomers in optimised conformation.

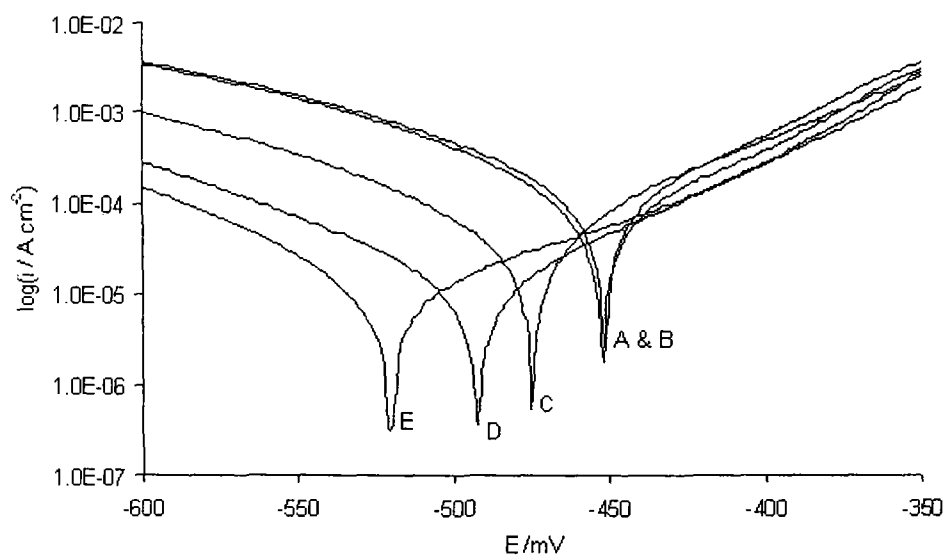


Fig. 5. The effect of concentration of mangrove tannin on the potentiodynamic curves of steel in 0.5 M HCl : A- HCl, B- 0.1 g/L tannin, C- 1.0 g/L tannin, D- 3.0 g/L tannin, E- 6.0 g/L tannin.

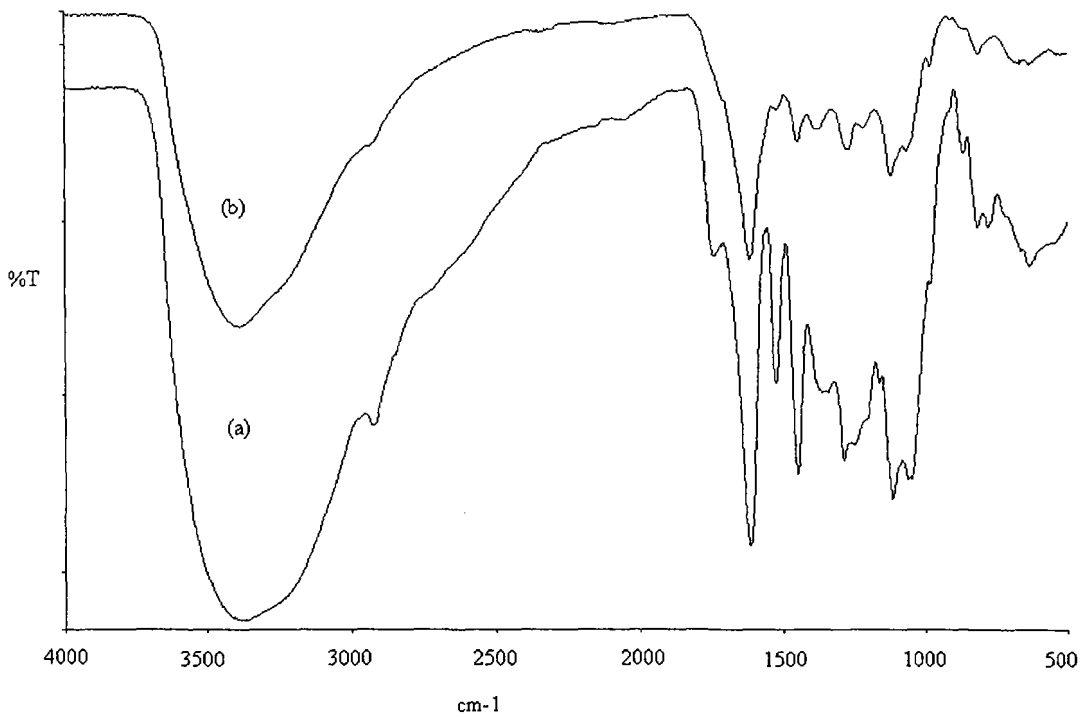


Fig. 6. FTIR spectrum of (a) tannin and (b) ferric-tannate synthesised at pH 4.0.

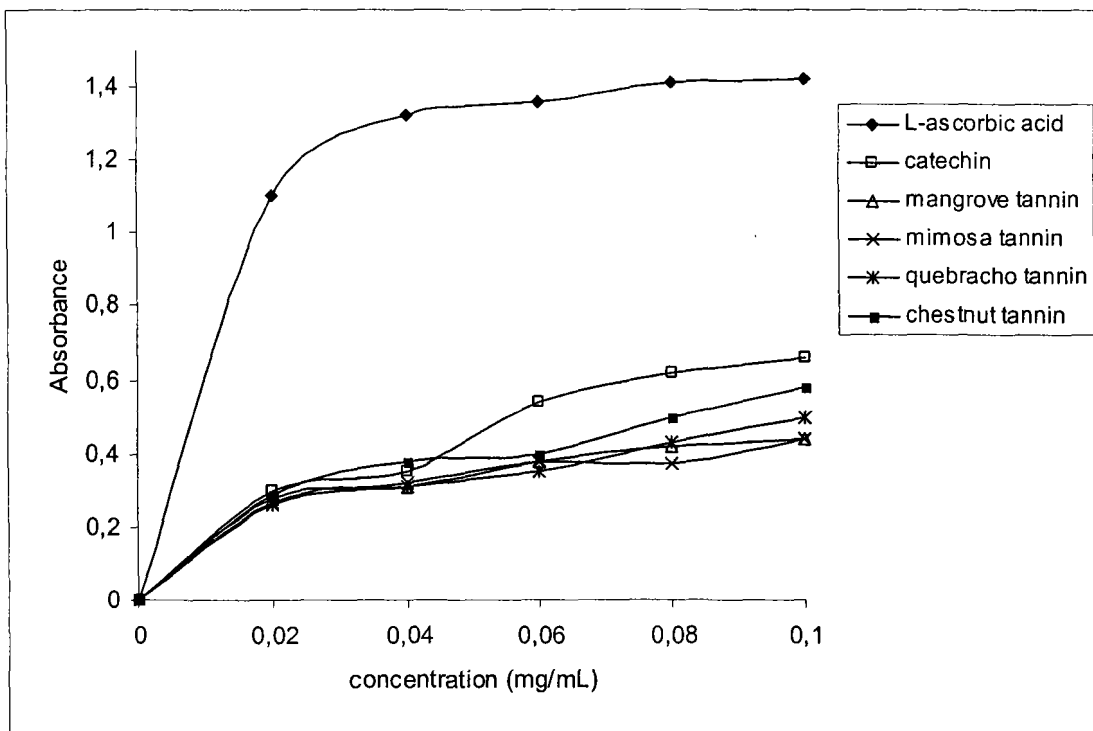


Fig. 7. Comparison of the reducing power of the various tannins with ascorbic acid and catechin standards.

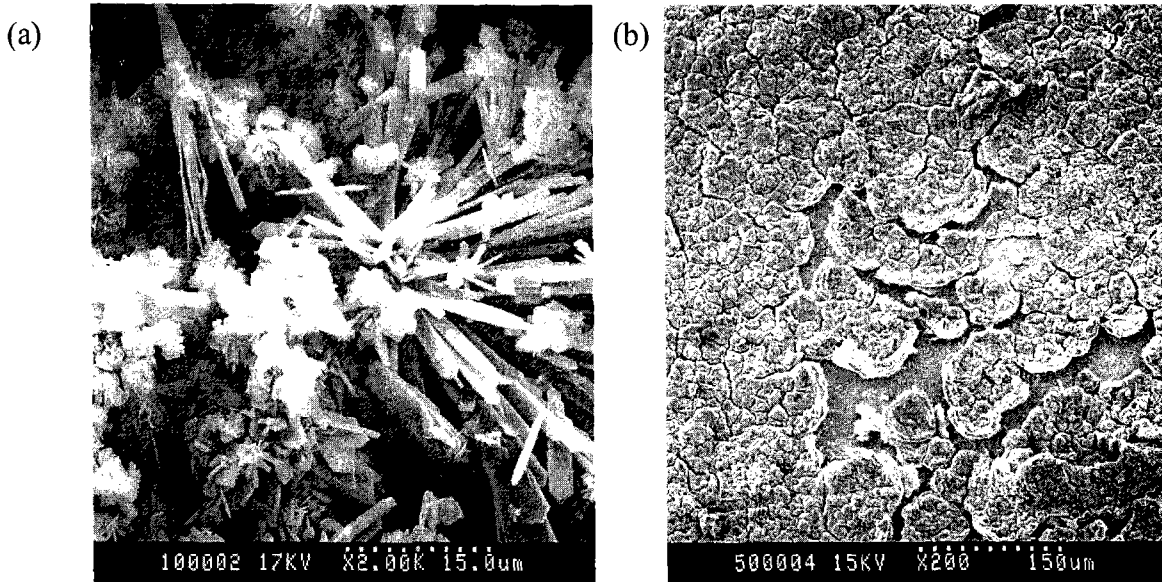


Fig.8. SEM micrographs of (a) pre-rusted sample (b) pre-rusted sample + 3g/L mangrove tannin treated for 24 hr at pH 4.0.

Table 1. Inhibition efficiency of steel corrosion at different concentrations of flavanoids based on polarisation resistance, R_p measurements in 0.5 M HCl (pH 0.5).

Flavanoid monomers	Concentration (M)	$IE(\%)$ (from R_p)
Catechin	2.5×10^{-3}	61
	5.0×10^{-3}	61.5
	1.0×10^{-2}	69.4
	5.0×10^{-2}	56.3
Epicatechin	2.5×10^{-3}	33.5
	5.0×10^{-3}	71.9
	1.0×10^{-2}	54.4
	5.0×10^{-2}	44.1
Epicatechin gallate	2.5×10^{-3}	73.6
	5.0×10^{-3}	61.8
	1.0×10^{-2}	55.4
Epigallocatechin	1.0×10^{-3}	0
	2.5×10^{-3}	44.1
	5.0×10^{-3}	55.4

Table 2. Comparison of the inhibition efficiency, $IE(\%)$ of steel in 0.5 M HCl (pH 0.5) containing the various concentrations of mangrove tannins.

Concentration of mangrove tannins (g/L)	$IE(\%)$ (from Tafel curve)	$IE(\%)$ (from R_p)
0.1	0	0
1.0	66.9	66.7
3.0	88.2	87.9
6.0	92.1	89.9

Table 3. Comparison of the inhibition efficiency, $IE(\%)$ of steel in HCl at pH 0, 0.5, 2.0 and 4.0 containing 3 g/L of the various tannins investigated.

	$IE(\%)$ (from Tafel curve)	$IE(\%)$ (from R_p)
pH=0		
Mangrove tannin	87.9	84.5
Mimosa tannin	97.6	94.1
Quebracho tannin	95.5	94
Chestnut tannin	97.2	96.3
Condensed tannin of mangrove	82.4	79.6
pH=0.5		
Mangrove tannin	88.2	87.4
Mimosa tannin	96.2	95.4
Quebracho tannin	80.2	86.3
Chestnut tannin	87.9	84.2
Condensed tannin of mangrove	82.0	68.2
pH=2.0		
Mangrove tannin	71.6	68.2
Mimosa tannin	82.3	80.5
Quebracho tannin	54.8	57.6
Chestnut tannin	28.2	17.6
Condensed tannin of mangrove	62.1	46.6
pH=4.0		
Mangrove tannin	44.2	21.9
Mimosa tannin	0	0
Quebracho tannin	0	0
Chestnut tannin	0	0
Condensed tannin of mangrove	41.2	0

Figure captions

Fig. 1. Chemical structure of flavanoid monomers that constitute mangrove tannin.

Fig. 2. Potentiodynamic curves of steel in 0.5 M HCl containing various concentrations of (a) catechin, (b) epicatechin, (c) epicatechin gallate and (d) epigallocatechin: A- HCl solution, B- 2.5×10^{-3} M, C- 5.0×10^{-3} M, D- 1.0×10^{-2} M, E- 5.0×10^{-2} M.

Fig. 3. Variation of polarisation resistance, R_p with time of immersion containing (a) 2.5×10^{-3} M, (b) 5.0×10^{-3} M and (c) 1.0×10^{-2} M flavanoids in 0.5 HCL.

Fig. 4. HOMO density as an isosurface for (a) catechin, (b) epicatechin and (c) epigallocatechin monomers in optimised conformation.

Fig. 5. The effect of concentration of mangrove tannin on the potentiodynamic curves of steel in 0.5 M HCl : A- HCl, B- 0.1 g/L tannin, C- 1.0 g/L tannin, D- 3.0 g/L tannin, E- 6.0 g/L tannin.

Fig. 6. FTIR spectrum of (a) tannin and (b) ferric-tannate synthesised at pH 4.0.

Fig. 7. Comparison of the reducing power of the various tannins with ascorbic acid and catechin standards.

Fig.8. SEM micrographs of (a) pre-rusted sample (b) pre-rusted sample + 3g/L mangrove tannin treated for 24 hr at pH 4.0.

Fig. 9. Variation of polarisation resistance, R_p with time of immersion in HCl solution at pH 4.0 containing 3 g/L of different tannins.

Table 1. Inhibition efficiency of steel corrosion at different concentrations of flavanoids based on polarisation resistance, R_p measurements in 0.5 M HCl (pH 0.5).

Table 2. Comparison of the inhibition efficiency, $IE(\%)$ of steel in 0.5 M HCl (pH 0.5) containing the various concentrations of mangrove tannins.

Table 3. Comparison of the inhibition efficiency, $IE(\%)$ of steel in HCl at pH 0, 0.5, 2.0 and 4.0 containing 3 g/L of the various tannins investigated.